Aust. J. Phys., 1987, **40**, 847–54

Correlation Properties of a Short Scale Microstructure of Pulsar Radio Emission within a 100 kHz Bandwidth*

L. I. Gurvits,[A] *O. A. Kuzmin,*[A] *M. V. Popov*[A] *and T. V. Smirnova*[B]

[A] Space Research Institute, USSR Academy of Sciences,
Profsojuznaya 84/32, 117810, Moscow, USSR.
[B] Lebedev Physical Institute, USSR Academy of Sciences,
Pushchino Radio Astronomical Station, 142292, Pushchino, USSR.

Abstract

The correlation of a radio emission microstructure of pulsars PSR 0809+74, PSR 0950+08 and PSR 1133+16 within a 100 kHz bandwidth at frequency 100 MHz has been investigated. It is shown that PSR 0809+74 and PSR 1133+16 micropulse structure shorter than $\sim$400 μs is not retained for a 50 kHz frequency offset. The microstructure longer than 500 μs is highly correlated inside a 100 kHz bandwidth for PSR 0809+74 and PSR 1133+16. For PSR 0950+08, micropulses longer than $\sim$150 μs are correlated over the same range. So, for PSR 0809+74 and PSR 1133+16 the short scale micropulse (t_μ < 400 μs) emission is narrowed (i.e. the normalised bandwidth $\Delta f/f_0$ of the short scale micropulses is less than 5×10^{-4}).

1. Introduction

Intensity variations of pulsar radio emission have a wide range of time scales. There are variations associated with the pulsar rotation, and temporal modulations within the emission time window (the so-called subpulses); within subpulses the emission is modulated by micropulses. Each type of variability has a certain emission bandwidth. For PSR 1133+16 microstructure with $\sim$550 μs the characteristic time has a high correlation at frequencies separated by up to 1 GHz (Boriakoff and Ferguson 1980), but micropulses shorter than $\sim$350 μs have an emission bandwidth less than 1·6 MHz (Smirnova *et al.* 1986).

It was shown (Popov *et al.* 1985) for PSR 0809+74 and PSR 1133+16 that micropulses with duration $\geqslant$400 μs are well correlated between frequencies 70 and 102·5 MHz, but shorter micropulses do not correlate for a frequency offset of 1·6 MHz (Smirnova *et al.* 1986). For PSR 0950+08, microstructure with a time scale $\sim$200 μs is well correlated at frequencies separated by up to 1 GHz (Boriakoff and Ferguson 1980), but shorter micropulses (t_μ < 100 μs) do not correlate for a frequency offset of $\sim$20 MHz (Popov *et al.* 1985).

The dependence of emission bandwidth on microstructure duration makes it possible to recognise the two types of microstructure: short scale (t_μ < 400 μs) and large scale (t_μ > 400 μs) (Smirnova *et al.* 1986). The emission bandwidth of the large scale microstructure is at least a few tens of MHz, or in other words, the relative bandwidth is $\Delta f/f_0 \geqslant 0\cdot2$ (where Δf is the emission bandwidth and f_0 the

* Paper presented at the Joint USSR–Australia Shklovskii Memorial Symposium on Supernova Remnants and Pulsars, held at Pushchino, USSR, 8–11 June 1986.

0004-9506/87/060847$02.00

emission central frequency), while $\Delta f/f_0 < 2\times10^{-2}$ for short scale microstructure at 102·5 MHz. There are several reasons to suggest that the short scale microstructure itself is closely related to the radio emission mechanism of the pulsar.

In this paper we investigate the short scale microstructure emission bandwidth with higher frequency resolution. For this purpose, a comparative analysis of the microstructure was carried out for two close frequency bands from $f_0-\frac{1}{2}B$ to f_0 and from f_0 to $f_0+\frac{1}{2}B$. Here f_0 is the central frequency about 100 MHz and B = 100 kHz is the receiving bandwidth. The temporal fine structure of the emission will be equal in both frequency intervals, if the microstructure emission bandwidth Δf is greater than the frequency offset between the intervals δf, or different if $\Delta f < \delta f$. Data for three pulsars were analysed: PSR 0809+74, PSR 0950+08 and PSR 1133+16. Each pulsar has micropulse emission; the micropulse durations are non-randomly distributed over a wide range of time scales from $\lesssim 50\ \mu$s to a few ms (Soglasnov *et al.* 1981, 1983).

2. Observations and Data Reduction

Our analysis is based on observations of PSR 0809+74, PSR 0950+08 and PSR 1133+16 carried out in 1978–81 with the BSA array (Vitkevich *et al.* 1976) at the Pushchino Radio Astronomy Station of the Lebedev Physical Institute. The high frequency signal from the pulsar was digitised and written on magnetic tape. Only pulses with a signal-to-noise ratio exceeding 10 were selected for the subsequent processing.

The data were then processed as follows:

(1) The time smearing due to the interstellar signal dispersion was removed by the pre-detection technique (Kardashev *et al.* 1978).

(2) Signal spectrum distortions due to the irregularity of the receiver bandpass were corrected.

(3) A complex Fourier spectrum of the pulsar signal was divided into two, the first from 0 to 50 kHz and the second from 50 to 100 kHz.

(4) The pulsar signal envelopes were restored in three frequency bands: band 1 [0–50 kHz, $x_1(t)$], band 2 [50–100 kHz, $x_2(t)$] and the full band 3 [0–100 kHz, $x_\Sigma(t)$]. Time resolution of 30 and 15 μs was achieved for pulses restored from the 50 and 100 kHz bands respectively.

(5) Individual autocorrelation functions (ACFs) for the subpulse intensity for signals in the three bands were computed and designated as $R_1(\tau)$, $R_2(\tau)$ and $R_\Sigma(\tau)$ respectively.

(6) The individual cross-correlation functions (CCFs) $R_{1/2}(\tau)$ between pulses at the two frequencies shifted on 50 kHz were also computed.

(7) The average ACFs $\langle R_1(\tau)\rangle$, $\langle R_2(\tau)\rangle$ and $\langle R_\Sigma(\tau)\rangle$ and the CCFs $\langle R_{1/2}(\tau)\rangle$ were computed by summing the corresponding individual ACFs and CCFs.

3. Analysis Technique

The analysis of spectral properties of the pulsar radio emission microstructure was carried out in two steps. The first step consists of a visual comparison of the temporal structure of pulses in the different frequency bands. We were able to obtain useful qualitative information by this inspection.

For the second step individual CCFs between $x_1(t)$ and $x_2(t)$ were analysed for the following: (1) the presence of the short scale structure correlation; (2) the value of this time scale t_μ (estimated from breakpoint in the CCF); (3) the value of the correlation coefficient; and (4) the lag of maximum correlation.

Individual CCFs were analysed together with individual ACFs. This analysis is required because the existence of the correlation feature itself is not firm evidence that the investigated processes in pulses $x_1(t)$ and $x_2(t)$ have something in common. Even for independent records containing microstructure of the same width t_μ, in some cases the individual CCF also will contain the correlation feature t_μ, but in this case the position of lag of maximum of the feature will be random. If microstructure at the two frequencies is correlated, then the microstructure cross-correlation peak should be at zero lag and the CCF and both ACFs must have the same t_μ.

In the average CCF and ACF the microstructure feature is emphasised for a correlated process. If the microstructure is a wideband property (the bandwidth of emission is more than the difference between frequencies), then the average ACFs would be almost equal to the average CCF $\langle R_{1/2}(t)\rangle$, i.e. both must have the same microstructure features. For narrowband microstructure the accidental correlation features in the individual CCFs are added with the random lags τ, then the average CCF will show no microstructure feature near zero lag.

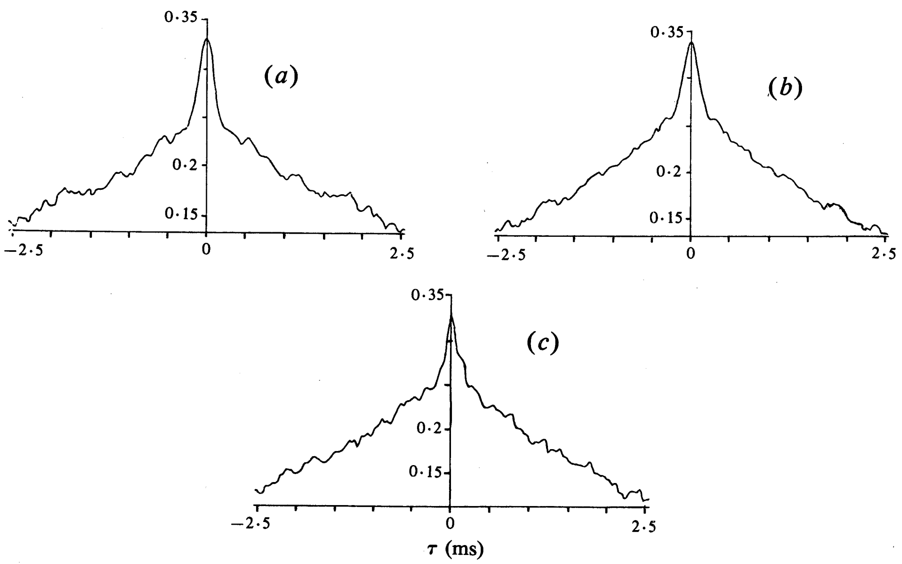

Fig. 1. Pulsar PSR 0950+08 and its average ACFs and CCF of the 63 pulses: (*a*) $\langle R_1(\tau)\rangle$ in the frequency band 1 (0–50 kHz); (*b*) $\langle R_2(\tau)\rangle$ in the frequency band 2 (50–100 kHz); and (*c*) average CCF between pulses in bands 1 and 2. The smoothing time is 20 μs in all figures.

4. Results

(a) PSR 0950+08

A total of 63 strong pulses were selected for analysis. The microstructure with a characteristic time scale $\sim$150 μs is very prominent in the average ACFs $\langle R_1(\tau)\rangle$

and $\langle R_2(\tau)\rangle$ (see Figs 1*a* and 1*b*). Analysis of this structure in the frequency bands 1 and 2, carried out as described above, shows their visual resemblance [the pulses $x_1(t)$, $x_2(t)$ and $x_\Sigma(t)$ are shown in Fig. 2*c*] and the existence of correlation features at $\sim 150\ \mu s$ in an individual CCF (see Fig. 2*d*) and the average CCF (see Fig. 1*c*). So for PSR 0950+08, microstructure with $\gtrsim 150\ \mu s$ characteristic time is correlated over a bandwidth of $\geqslant 50$ kHz.

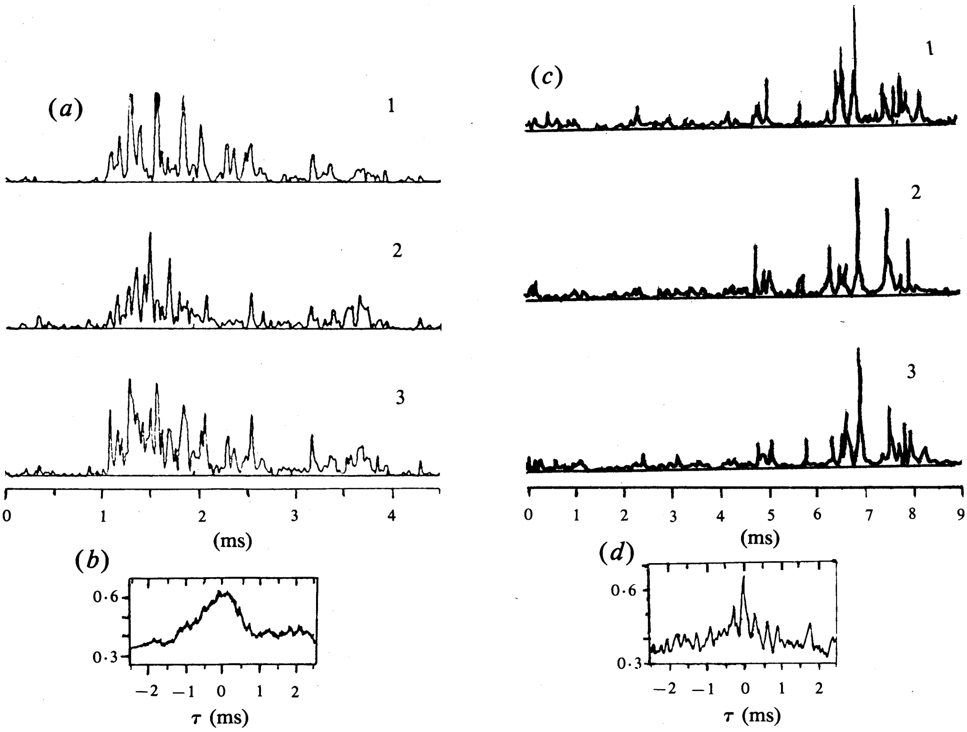

Fig. 2. A single pulse of (*a*) PSR 1133+16 and (*c*) PSR 0950+08 in the frequency bands 1, 2 and 3 (where 3 is the full band 0–100 kHz). The corresponding individual CCFs are shown in (*b*) and (*d*).

(b) PSR 0809+ 74 and PSR 1133+ 16

The fine structure analysis of the pulses in two close frequency bands was performed for PSR 0809+74 and PSR 1133+16 in the same way as for PSR 0950+08. First, pulses corresponding to the frequency bands 1 and 2 were visually compared. Such a qualitative comparison has shown a certain resemblance between temporal structures on time scales of $\gtrsim 0\cdot 6$ ms.

Nevertheless, more short scale micropulse morphology has little in common in the two bands. PSR 1133+16 and PSR 0809+74 pulses, corresponding to the frequency bands 1, 2 and 3 shown in Figs 2*a* and 3*a*, illustrate this claim. Both figures demonstrate that the short scale micropulse ($t_\mu \simeq 200\ \mu s$) structure differs markedly in the two bands.

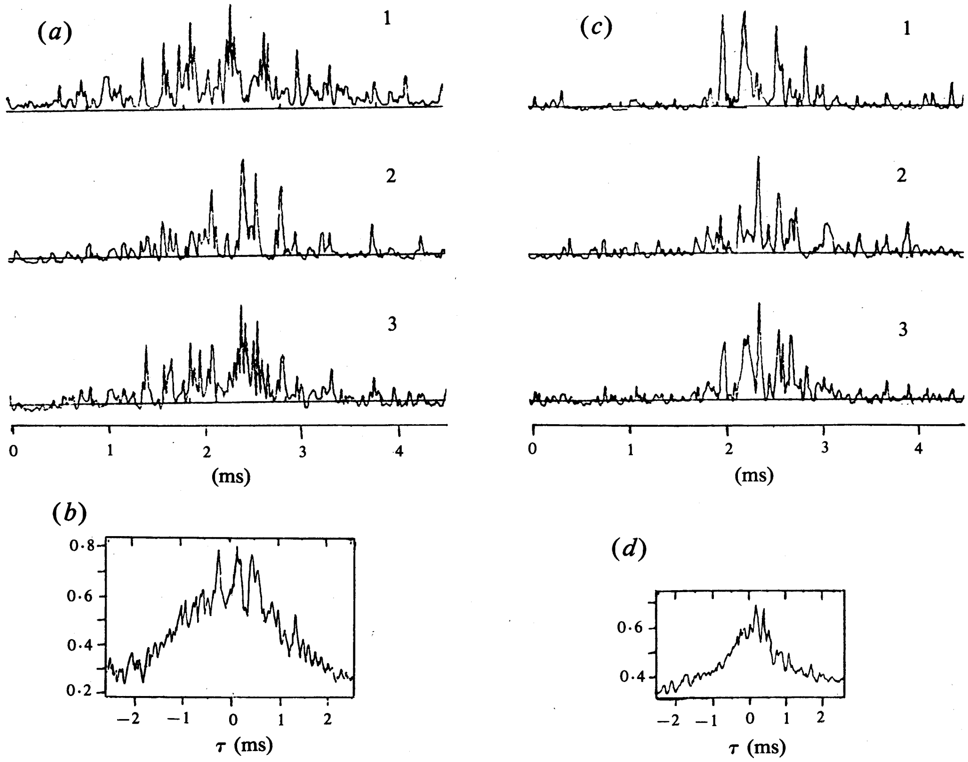

Fig. 3. As for Fig. 2 but for (*a*) PSR 0809+74 and (*c*) PSR 1133+16; the corresponding CCFs are given in (*b*) and (*d*).

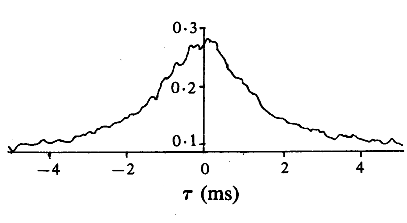

Fig. 4. Average CCF for PSR 1133+16 for the different pairs of 25 kHz frequency bands (the CCF was averaged over 50 pulses).

The correlation analysis of the individual pulses was performed on the basis of 91 pulses for PSR 0809+74 and 67 pulses for PSR 1133+16. The analysis has shown that either CCFs contain short scale microstructure features ($t_\mu \lesssim 400\ \mu$s), corresponding to the ACFs features, but with correlation maxima positions being randomly distributed around zero lag or with short scale microstructure feature absent. Fig. 2*b* shows an example of the PSR 1133+16 individual CCF, where the short scale microstructure feature is absent. Another example of the PSR 0809+74 individual CCF, shown in Fig. 3*b*, demonstrates the case where the microstructure correlation feature is shifted from zero lag to $\tau = 200\ \mu$s.

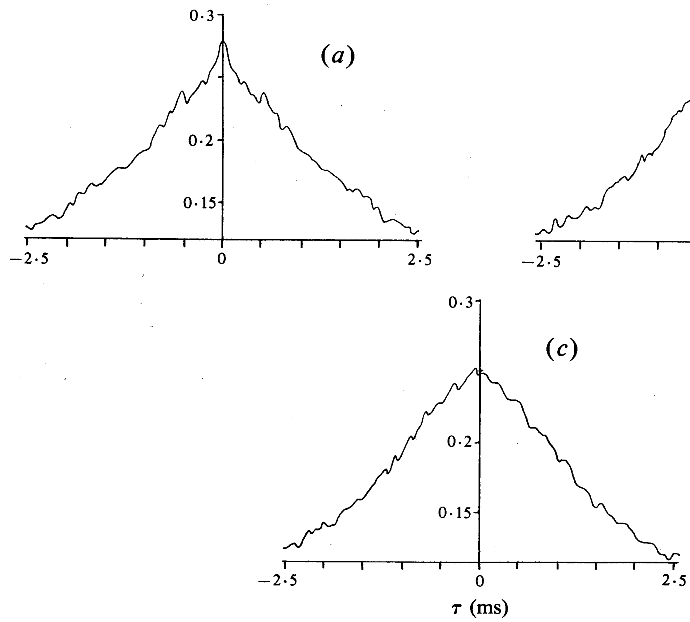

Fig. 5. Average ACFs of PSR 0809+74 from pulses in: (*a*) band 1; (*b*) band 2; and (*c*) average CCF from pulses in bands 1 and 2. Both ACFs and CCF were averaged over 91 pulses.

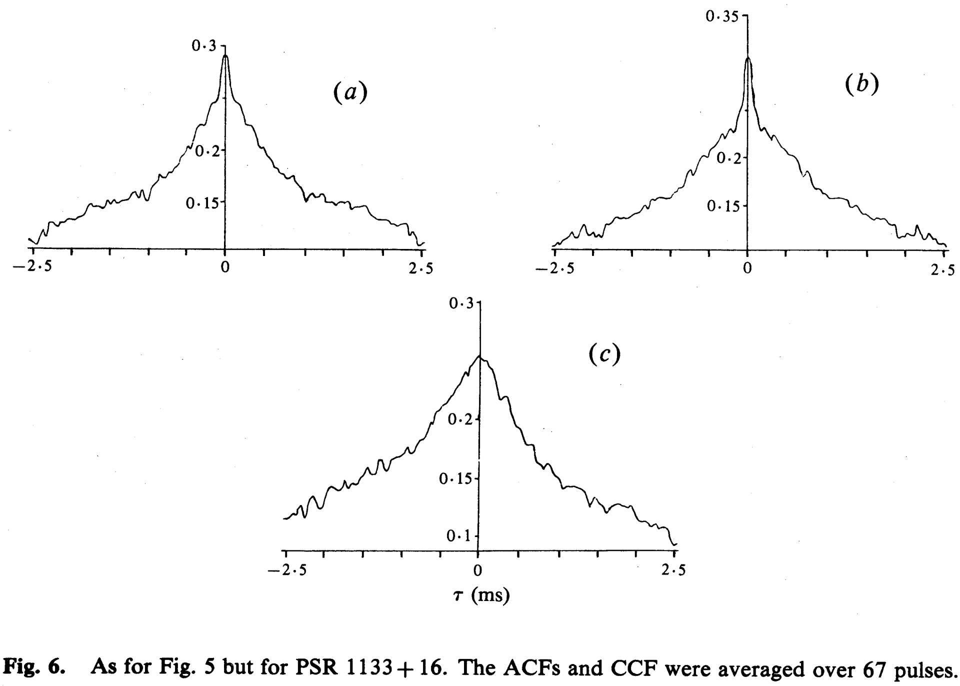

Fig. 6. As for Fig. 5 but for PSR 1133+16. The ACFs and CCF were averaged over 67 pulses.

For PSR 1133+16, short scale microstructure correlation within a narrower frequency band was analysed. For this pulsar the 100 kHz complex Fourier spectra were divided into four adjacent frequency bands each of 25 kHz. In this case the data processing and the analysis technique were the same as those for two bands. The effective time resolution was 60 μs. In this case the structure of micropulses of $\sim$150 μs time duration differs markedly even for a 25 kHz frequency offset. Also, the lags of correlation maxima are randomly distributed. Fig. 4 shows that the average CCF for PSR 1133+16 between pulses in frequency bands shifted on 25 kHz has no correlation features shorter than $\sim$700 μs.

To improve the reliability of the correlation analysis, the average ACFs and CCFs were computed. Average CCFs of PSR 0809+74 (Fig. 5*c*) and PSR 1133+16 (Fig. 6*c*) obviously do not display any prominent microstructure features shorter than $\sim$1·4 ms and $\sim$600 μs respectively. For both pulsars the average ACFs indicate the presence of microstructure features with $t_\mu \approx 1{\cdot}3$ ms and $\sim$700 μs respectively. There is also a short scale feature with $t_\mu \sim 70$ μs in the ACFs of these pulsars. Evidently microstructure features of $\sim$70 μs width are absent in the average CCFs.

5. Possible Propagation Effects in the Interstellar Medium

Let us consider whether propagation through the interstellar medium can cause the observed absence of short scale microstructure correlation in the 100 kHz bandwidth for PSR 0809+74 and PSR 1133+16. Two main effects can alter the frequency–time structure of the pulsar signals: scattering by inhomogeneities in the interstellar electron distribution and Faraday rotation of the plane of polarisation of a linearly polarised wave. The scattering process causes decorrelation of the pulsar radio signal across the receiver bandpass with a decorrelation bandwidth $\Delta\nu_p$ characteristic of each pulsar. Measured decorrelation bandwidths for PSR 0809+74, PSR 0950+08 and PSR 1133+16 are 130±30, 210±50 and 9·1±3·0 kHz respectively at a central frequency of 105 MHz (Shitov 1972). A value of $\Delta\nu_p < 90$ kHz was also obtained for PSR 1133+16 at 112 MHz (Ewing *et al.* 1971). Decorrelation bandwidths $\Delta\nu_p$ for PSR 0809+74 and PSR 0950+08 are greater than the recording receiver bandwidth $B = 100$ kHz and so scattering has no influence on short scale microstructure correlation at two frequencies 50 kHz apart. For PSR 1133+16, $B > \Delta\nu_p$ and the scattering effect has to be considered. However, this effect only causes slow modulation of short scale microstructure emission and it could not lead to the observed absence of microstructure correlation at two close frequencies.

Since only one linearly polarised component of pulsar radio emission was recorded in our observations, it is necessary to consider the effect of Faraday rotation of the plane of polarisation across the receiver bandwidth. The differential rotations across the 100 kHz bandwidth at 100 MHz are 0·21, 0·02 and 0·07 rad for PSR 0809+74, PSR 0950+08 and PSR 1133+16 respectively. Thus, total changes of the direction of the plane of polarisation for all three pulsars are small enough and do not cause a significant effect on the frequency structure of the received pulsar signal.

6. Conclusions

First of all let us summarise our main experimental findings:

(1) Short scale microstructure with a duration of $\lesssim$400 μs is not retained for a frequency offset 50 kHz at the central frequency $\sim$100 MHz for two of the

three pulsars investigated, PSR 0809+74 and PSR 1133+16; for PSR 0950+08 the structure of micropulses with duration $\gtrsim 150\ \mu s$ is the same in the frequency band 100 kHz.

(2) The large scale microstructure ($t_\mu \gtrsim 500\ \mu s$) is correlated within the 100 kHz frequency band at ~ 100 MHz central frequency for all pulsars investigated.

So, for pulsars PSR 0809+74 and PSR 1133+16 short scale micropulse emission is narrowband (the normalised bandwidth of emission is $\Delta f/f_0 \leqslant 5\times10^{-4}$). To obtain this low value of $\Delta f/f_0$ in the framework of the 'antenna-like' coherent radio emission mechanism (Benford and Bushauer 1977), the emission wavelength and the emitting system dimension s must be related as $\lambda/s \leqslant 5\times10^{-4}$. Thus, we obtain a lower limit to the dimension of $s \geqslant 10^6$ cm for $\lambda = 3\times10^2$ cm, corresponding to the 100 MHz central frequency.

For PSR 0950+08, micropulses with duration $\sim 150\ \mu s$ correlate at frequencies separated by up to 1 GHz, but for the other two pulsars such a correlation is absent even with the frequency offset of $\delta f = 50$ kHz.

A comparison of micropulse durations, expressed in degrees, shows that for PSR 0950+08 the duration of wideband micropulses $0^\circ\!\cdot\!28$ ($t_\mu \sim 200\ \mu s$) is nearly the same as the time scales of wideband micropulses: $0^\circ\!\cdot\!36$ ($\sim 1\cdot3$ ms) for PSR 0809+74 and $0^\circ\!\cdot\!18$ ($\sim 600\ \mu s$) for PSR 1133+16. This can be explained by the linear dependence of wideband micropulse width with pulsar period. If micropulses are due to temporal modulation of the emission region in connection with modulation of particle injection at the stellar surface, which depends on the rotation-generated electric field, a variation with pulsar period of micropulse duration may be expected.

Acknowledgments

We are grateful to A. Yu. Novikov and V. A. Soglasnov for help with observations and A. A. Bocharov, N. S. Kardashev, S. V. Pogrebenko and T. L. Orlova for valuable help and encouragement.

References

Benford, G., and Bushauer, R. (1977). *Mon. Not. R. Astron. Soc.* **179**, 189.

Boriakoff, V., and Ferguson, D. C. (1980). IAU Symp. No. 95, p. 191 (Reidel: Dordrecht).

Ewing, M. S., Batchelor, R. A., and Friefeld, R. (1971). IAU Symp. No. 46, p. 129 (Reidel: Dordrecht).

Kardashev, N. S., Kuzmin, A. D., Nikolaev, N. Ya., Novikov, A. Yu., Popov, M. V., Smirnova, T. V., Soglasnov, V. A., Shabanova, T. V., Shinskii, M. D., and Shitov, Yu. P. (1978). *Astron. Zh.* **55**, 1024.

Popov, M. V., Smirnova, T. V., and Soglasnov, V. A. (1985). Preprint FIAN No. 288.

Shitov, Yu. P. (1972). *Astron. Zh.* **49**, 470.

Smirnova, T. V., Soglasnov, V. A., Popov, M. V., and Novikov, A. Yu. (1986). *Astron. Zh.* **63**, 84.

Soglasnov, V. A., Popov, M. V., and Kuzmin, O. A. (1983). *Astron. Zh.* **60**, 293.

Soglasnov, V. A., Smirnova, T. V., Popov, M. V., and Kuzmin, A. D. (1981). *Astron. Zh.* **58**, 771.

Vitkevich, V. V., Glushaev, A. A., Iljasov, Yu. P., Kutuzov, S. M., Kuzmin, A. D., Alekseev, I. A., Bunin, V. D., Novojenov, G. F., Solomin, N. S., and Tjaptin, M. M. (1976). *Radiophysica* **19**, 1594.

Manuscript received 19 March, accepted 19 October 1987